



## Effect of interfacial heat exchange on thermocapillary flow in a cylindrical liquid bridge in microgravity

Bo Xun<sup>a</sup>, Kai Li<sup>a,\*</sup>, Wen-Rui Hu<sup>a</sup>, Nobuyuki Imaishi<sup>b</sup>

<sup>a</sup>Key Laboratory of Microgravity (National Microgravity Laboratory), Institute of Mechanics, Chinese Academy of Sciences, Beijing 100190, China

<sup>b</sup>Institute for Materials Chemistry and Engineering, Kyushu University, Kasuga 816-8580, Japan

### ARTICLE INFO

#### Article history:

Received 9 October 2009

Received in revised form 19 January 2011

Accepted 24 January 2011

#### Keywords:

Liquid bridge

Interfacial heat exchange

Thermocapillary flow

Critical Marangoni number

### ABSTRACT

The effect of interfacial heat exchange on thermocapillary flow in a cylindrical liquid bridge of 1 cst silicone oil (with Prandtl number 16.0) with aspect ratio 1.8 in microgravity, was investigated in an extended range of Biot number. With both constant and linearly distributed ambient temperature, the computed results predict that the marginal stability curve for the thermocapillary flow exhibits a roughly convex trend. In the range of small Biot number, however, a sharp local maximum exists with a special oscillation mode of azimuthal wave number  $m = 0$ , in contrast to the other cases with  $m = 1$ . In addition, the normalized “thermal” energy balance between the basic state and the critical perturbation of the thermocapillary flow was investigated. Finally, the effect of the interfacial heat exchange on the thermocapillary flow in a liquid bridge of low Prandtl number fluid in microgravity was investigated as a comparison.

© 2011 Elsevier Ltd. All rights reserved.

### 1. Introduction

A liquid bridge model consists of a liquid column floating between two differently heated solid rods (see Fig. 1). It was initially introduced to mimic half of the floating zone technique for space materials science [1], and has now become one of the typical models for the investigation, both experimentally and theoretically, of the principles of thermocapillary flow. Motivated by the experimental work of Chun and Wuest [2,3] and Schwabe et al. [4,5], extensive theoretical studies (e.g. linear instability analyses [6–9], energy stability analyses [10,11] and direct numerical simulations [12–14]) have established that an axisymmetric (2D) stationary thermocapillary flow first loses its stability to an asymmetric (3D) stationary flow, then to an oscillatory flow in liquid bridges of low Prandtl number fluids ( $Pr \leq 0.06$ ), while it transits to oscillatory flow directly in liquid bridges of higher Prandtl number fluids. However, the corresponding critical conditions determined through the theoretical studies do not give quantitative agreement with the experimental results, especially for high Prandtl number fluids. It should be noted that most of the theoretical studies were carried out with an adiabatic free-surface assumption, in other words there is no interfacial heat exchange on the free surface. In practice interfacial heat exchange in the experiments, especially under high temperature conditions, may play an important role in the fluid dynamics [15–20]. Kamotani et al.

[15,19] investigated experimentally the effect of interfacial heat exchange in liquid bridges of high Prandtl number fluids, taking into account the ambient air flow. They calculated the average interfacial heat transfer rate with respect to the dimensionless average Biot number ( $Bi$ ), and found that the critical Marangoni number decreased with increasing heat-loss to the environment in the range of average  $Bi$  less than 1.5, while the critical Marangoni number was only slightly affected by increasing heat-gain from the environment. Melnikov and Shevtsova [17] investigated numerically the effect of interfacial heat exchange on coupled thermocapillary flow and buoyancy flow in a cylindrical liquid bridge ( $Pr = 14$  and  $\Gamma = 1.8$ ) with a constant ambient temperature (the effect of free-surface deformation was ignored) [20]. They found that the heat-loss serves as a stabilizing effect on the flow at large  $Bi$  ( $Bi \geq 5$ ) contrary to the destabilizing effect at small  $Bi$  ( $Bi \leq 2$ ). Kousaka and Kawamura [18] studied numerically thermocapillary flow in a liquid bridge ( $Pr = 28.1$  and  $\Gamma = 1.0$ ) in microgravity with a linearly distributed ambient temperature. The destabilization of thermocapillary flow by interfacial heat-loss in the range of small  $Bi$  ( $Bi < 1$ ) was also found. However, due to the computational task of 3D direct numerical simulations, the results available in Ref. [18] are still fragmentary (there are only two data points in the range  $0 < Bi < 1$  where steep variation of the marginal curve occurs, according to the present study). However, with the aim of manipulation of oscillatory thermocapillary flow in a liquid bridge through external application of forced gas flow, which closely relates to the effect of interfacial heat exchange, a space experiment co-operated by ESA and JAXA researchers is scheduled in ISS in the

\* Corresponding author. Tel.: +86 10 82544098; fax: +86 10 82544096.

E-mail address: [likai@imech.ac.cn](mailto:likai@imech.ac.cn) (K. Li).

**Nomenclature**

$A$	matrix in eigenvalue problem	$T$	dimensionless temperature
$B$	matrix in eigenvalue problem	$T_0$	mean temperature of the upper and lower ends
$Bi = \frac{hR}{k}$	Biot number	$T_{amb}$	dimensionless ambient temperature
$D_{th}$	thermal dissipation	$T_{cold}$	dimensionless temperature on the cold rod
$E_{th}$	“thermal” energy of disturbances	$\vec{U} = (u, v, w)$	dimensionless velocity vector
$h$	heat transfer coefficient on free surface	$x$	vector composed of disturbance velocity, pressure and temperature $(u', iv', w', p', T')^T$
$h(z)$	free surface local radius	$X$	the basic steady axisymmetric state
$i$	$\sqrt{-1}$	$V_0$	the liquid volume with cylindrical shape
$J_i$	interactive term in “thermal” energy equation decomposed in cylindrical coordinates	<b>Greek symbols</b>	
$k$	thermal conductivity coefficient	$\alpha$	thermal diffusivity coefficient
$L$	height of the liquid bridge	$\beta$	thermal expansion coefficient
$Ma = \frac{\gamma \Delta T R}{\mu \alpha}$	Marangoni number	$\Delta T$	applied temperature difference
$\vec{n}$	the outward-directed normal vector of the free surface	$\gamma$	negative temperature gradient of surface tension
$N_z$	number of the grid points in axial direction	$\Gamma = \frac{l}{R}$	aspect ratio
$N_r$	number of the grid points in radial direction	$\mu$	dynamic viscosity coefficient
$P$	pressure	$\nu$	kinematic viscosity coefficient
$Pr = \frac{\nu}{\alpha}$	Prandtl number	$\rho_0$	mean density
$(r, \varphi, z)$	cylindrical coordinate	$\sigma(m)$	the complex growth rate of the corresponding perturbation mode
$R$	radius of the liquid bridge	$\mu$	dynamic viscosity coefficient
$S$	dimensionless stress tensor $S = \nabla \vec{U} + (\nabla \vec{U})^T$	$\Omega$	volume domain occupied by the liquid bridge
$t$	dimensionless time	$\varepsilon$	thermal radiation
$\vec{t}_\varphi$	the unit vector tangent to the free surface in the $(r, \varphi)$ plane		
$\vec{t}_z$	the unit vector tangent to the freesurface in the $(r, z)$ plane		

near future, and the corresponding preliminary theoretical studies are necessary due to the scarce space experiment opportunities. In the present study, linear stability analyses were conducted to investigate the dependency of the critical conditions of thermocapillary flow on interfacial heat exchange in a liquid bridge of a high Prandtl number fluid in microgravity, with both constant and linearly distributed ambient temperature. Moreover, the normalized “thermal” energy balance between the basic state and the critical perturbation of thermocapillary flow was investigated. Finally, the effect of interfacial heat exchange on thermocapillary flow in a liquid bridge of low Prandtl number fluid in microgravity was investigated as a comparison.

**2. Governing equations and numerical schemes**

Fig. 1 shows a schematic diagram of the liquid bridge of the 1 cst silicone oil ( $\Gamma = 1.8, Pr = 16.0$ ) adopted in the present study. The thermo-physical properties of the silicone oil are listed in

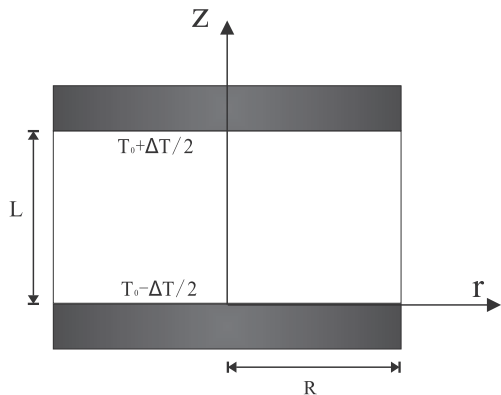


Fig. 1. Schematic of a cylindrical liquid bridge in microgravity.

Table 1. With the unitary volume ratio usually adopted in the space experiment, the liquid column is cylindrical. The length, velocity, pressure and time are scaled by  $R, \frac{\nu \Delta T}{\mu}, \frac{\gamma \Delta T}{R}$  and  $\frac{R^2}{\nu}$ , respectively. The temperature measured with respect to  $T_0$  is scaled by  $\Delta T$ . In the cylindrical coordinates  $(r, \varphi, z)$ , the non-dimensional governing equations are as follows:

$$\nabla \vec{U} = 0, \tag{1}$$

$$\frac{\partial \vec{U}}{\partial t} + \frac{Ma}{Pr} (\vec{U} \nabla) \vec{U} + \nabla P = \Delta \vec{U}, \tag{2}$$

$$\frac{\partial T}{\partial t} + \frac{Ma}{Pr} (\vec{U} \nabla) T = \frac{1}{Pr} \Delta T \tag{3}$$

The corresponding boundary conditions are as follows:

$$z = 0, \Gamma : \vec{U} = 0, T = \mp \frac{1}{2}, \tag{4}$$

$$r = 1 : \vec{n} \vec{U} = 0, \vec{t}_z S \vec{n} = -\vec{t}_z \nabla T, \vec{t}_\varphi S \vec{n} = -\vec{t}_\varphi \nabla T, \vec{n} \nabla T = -Bi(T - T_{amb}). \tag{5}$$

For the linear stability analysis, the basic axisymmetric steady state,  $X = \{\vec{U}(r, z) = U\vec{e}_r + W\vec{e}_z, P(r, z), T(r, z)\}$ , is first determined for a given set of parameters ( $Ma$  and  $Bi$ ). Then small three-dimensional disturbances are imposed on the basic state, and the corresponding equations are linearized by neglecting high orders of the disturbances. The disturbances are assumed to be in the normal modes:

Table 1 Thermophysical properties of 1 cst silicone oil.

$\rho_0$	818 (kg/m <sup>3</sup> )	$\beta$	0.00129 (K <sup>-1</sup> )
$\nu$	10 <sup>-6</sup> (m <sup>2</sup> /s)	$\gamma$	5.63 × 10 <sup>-5</sup> (kg/s <sup>2</sup> )
$K$	2.4 × 10 <sup>-2</sup> (cal/m · s · k)	Prandtl number	16.0

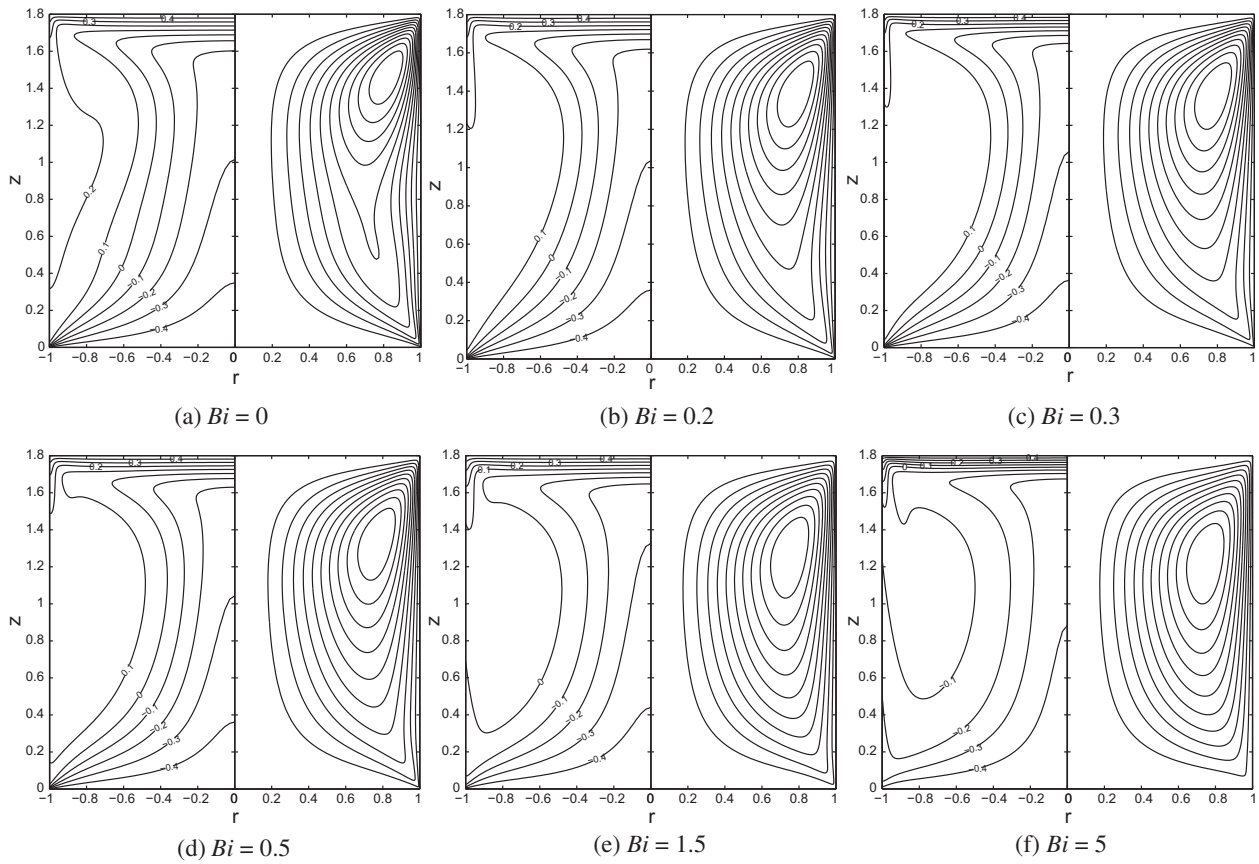


Fig. 2. Biot number dependent streamlines (right) and isotherms (left) of the basic steady flow at corresponding  $Ma_c$  for  $T_{amb} = -0.5$ .

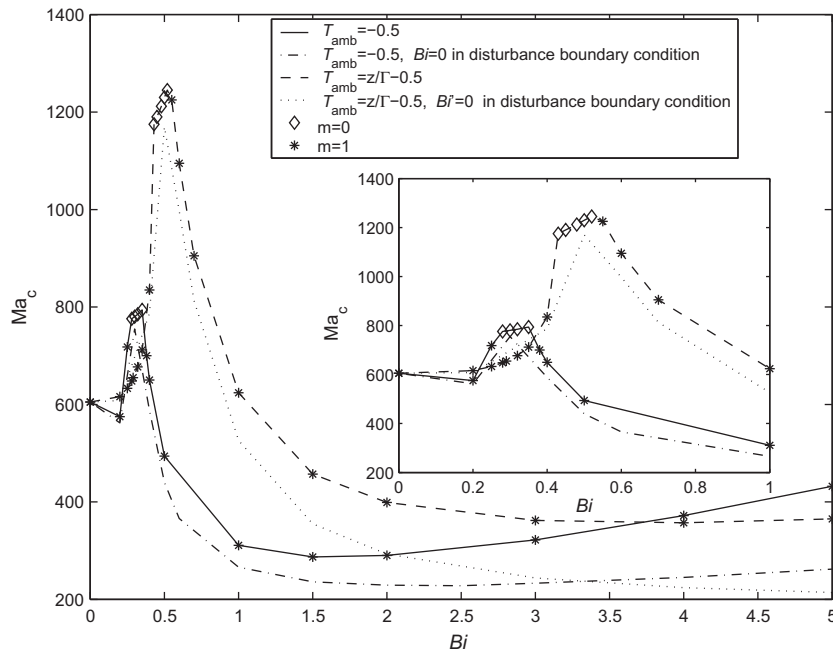


Fig. 3. Biot number dependent profiles of the critical Marangoni number.

$$\begin{pmatrix} \bar{u}' \\ P' \\ T' \end{pmatrix} = \sum_{m=-\infty}^{+\infty} \begin{pmatrix} \bar{u}^m(r, z) \\ p^m(r, z) \\ T^m(r, z) \end{pmatrix} \exp[\sigma(m)t + jm\phi]. \quad (7)$$

The discrete form of the linearized equations can be written as a generalized eigenvalue problem:

$$g(x, X, Ma, m, Bi) \equiv Ax = \sigma(m)Bx. \quad (8)$$

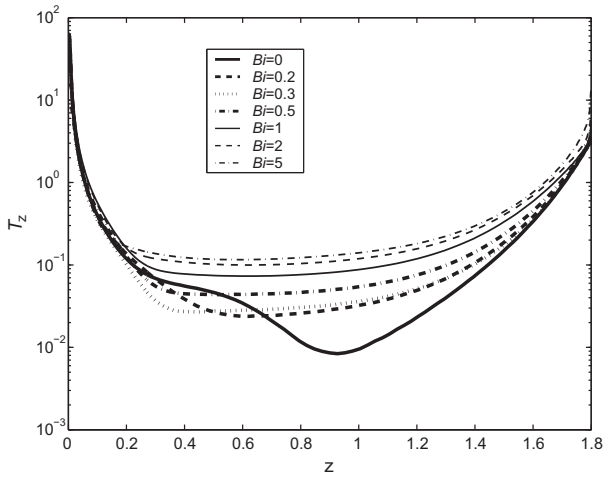


Fig. 4. Biot number dependent temperature gradient distribution at free surface at the corresponding  $Ma_c$  for  $T_{amb} = -0.5$ .

The eigenvalues and the related eigenfunctions of the problem are solved by the Arnoldi method [21]. For a non-symmetric eigenvalue problem, a direct method like QZ algorithm destroys the sparse structure of the problem and involves extensive computation task work which becomes impractical for large system. The Arnoldi method finds the desired eigenvalues through subspace iteration. Since we only concern about the extremal eigenvalue in our linear stability analysis, and the sparse structure of the problem, the Arnoldi method is a proper method to be adopted. And the success of its application has been demonstrated by our previous work [20,22]. The critical Marangoni number ( $Ma_c$ ) is obtained when the maximum of the real part of  $\sigma(m)$  for all  $m$  is zero. In practice, the azimuthal wave number  $m$  for the critical mode is not very large, and we calculated only for  $0 \leq m \leq 4$ . The details of the linear stability analysis can also be found in [22]. In order to properly resolve the boundary layers at both solid ends, a non-uniform mesh with denser grid points near the solid ends

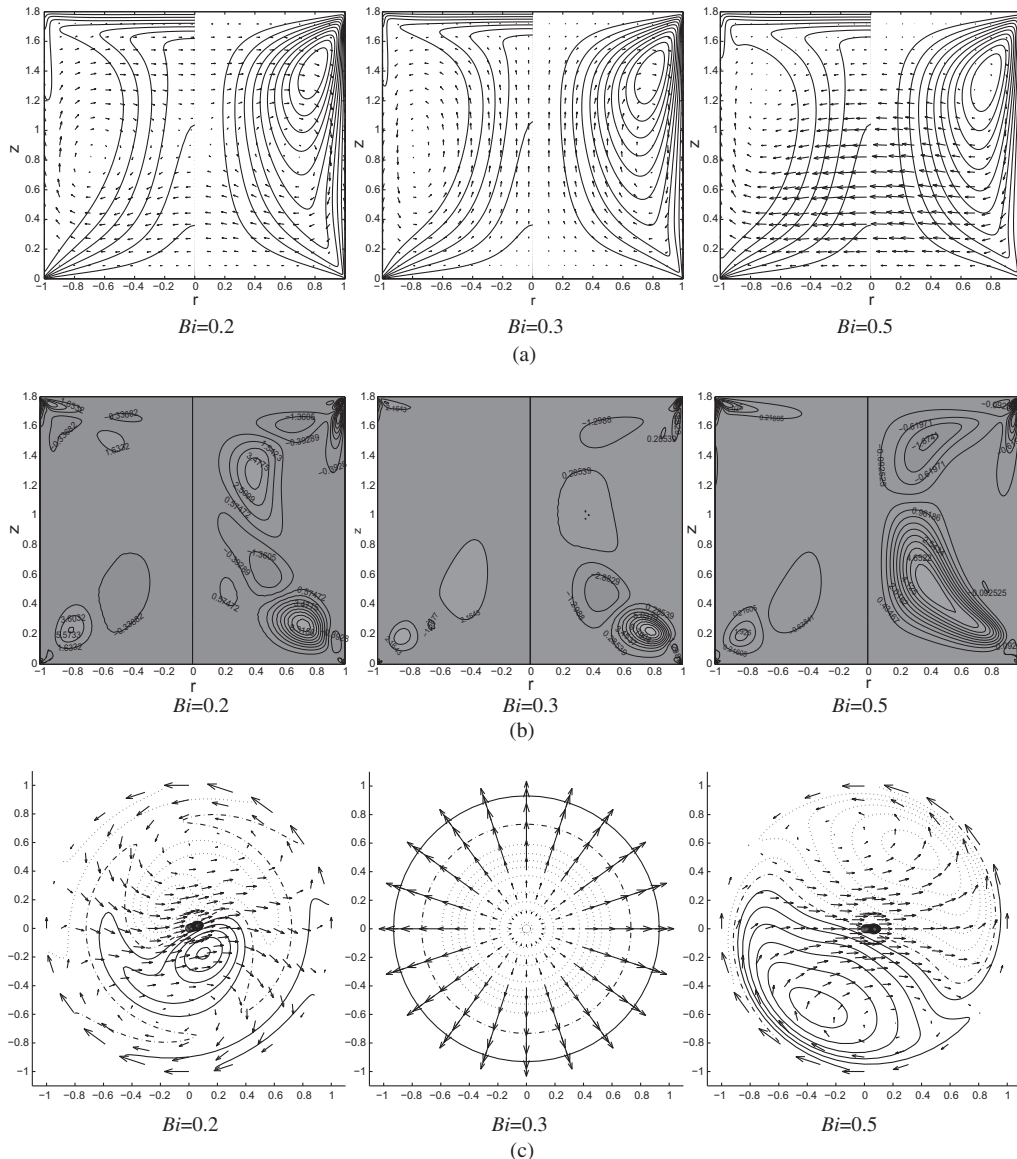


Fig. 5. (a) Streamlines (solid lines on right) and isothermals (solid lines on left) of the basic steady flow and velocity disturbances (vectors) in  $r$ - $z$  plane; (b) distribution density  $j_1$  (right) and  $j_2$  (left) in  $r$ - $z$  plane; (c) velocity disturbances (vectors) and isolines of temperature disturbances (solid lines: positive temperature disturbance; dotted lines: negative temperature disturbance; dash-dotted line: zero temperature disturbance.) at horizontal cut plane  $z = \frac{1}{2}$  at the corresponding critical state at different Biot number for  $T_{amb} = -0.5$ .

and the free surface was adopted in this study. The total grid number is  $N_r \times N_z = 81 \times 141$ . The detailed code validation can be found elsewhere [20,22].

To better understand the energy balance between the basic state of thermocapillary flow and the critical temperature perturbation, the rate of “thermal” energy change ( $E_{th}$ ) of the critical disturbance [7,9,10] was investigated: the thermal disturbance equation was multiplied by the temperature disturbance and integrated over the volume of the liquid bridge ( $\Omega$ ),

$$\frac{1}{D_{th}} \frac{dE_{th}}{dt} = Q + J - 1, \tag{9}$$

where  $E_{th} = \int_{\Omega} \frac{T'^2}{2} d\Omega$ ,  $D_{th} = \int_{\Omega} \frac{\nabla T' \nabla T'}{Pr} d\Omega$ . Note that Eq. (9) is normalized by the thermal dissipation ( $D_{th}$ ).  $Q = -\frac{Bi}{PrD_{th}} \oint_s T'^2 ds$  is the transport of “thermal” energy through the free surface,  $J = -\frac{Ma_c}{PrD_{th}} \int_{\Omega} (\vec{u}' \nabla T) T' d\Omega = J_1 + J_2 = -\frac{Ma_c}{PrD_{th}} \int_{\Omega} (u' \frac{\partial T}{\partial r}) T' d\Omega - \frac{Ma_c}{PrD_{th}} \int_{\Omega} (w' \frac{\partial T}{\partial z}) T' d\Omega$  is the interactive term between the basic thermal state and the disturbance, which indicates the energy transfer from the basic thermal field to the temperature disturbance field by the disturbance velocity. Moreover, the distribution density of  $J_1$  and  $J_2$  can be introduced as  $j_1$  and  $j_2$  through  $J_1 = \int_0^1 dz \int_0^1 j_1 dr$  and  $J_2 = \int_0^1 dz \int_0^1 j_2 dr$ . A similar procedure can be used for kinetic energy balance [10,20]. However, the thermal energy balance is the focus for the liquid bridge of high Prandtl number fluids as in the present study [10].

### 3. Results and discussion

We studied the thermocapillary flow in a cylindrical liquid bridge in microgravity with heat transfer through the free surface. First, the case with constant ambient temperature ( $T_{amb} = T_{cold}$ ) [17] was investigated. Fig. 2 shows the isotherms and streamlines of the basic steady axisymmetric field at the critical state for different Biot number. The isotherms crowd at the cold corner and nearly linearly distribute at the hot end except in the hot corner. In this case, the interfacial heat transfer is always heat-loss from the liquid bridge to the environment. The interfacial heat exchange pulls up the isotherms at the cold corner and enhances the axial temperature gradient at the hot end. Fig. 3 shows the Biot number dependent critical Marangoni number. In the range of intermediate and large  $Bi$ , the profile of the critical Marangoni number exhibits a convex trend, i.e. the critical Marangoni number firstly decreases with increasing Biot number up to  $Bi = 1.5$ , followed by an approximately linear increase. However, in the parameter range studied, the effect of heat-loss is not sufficiently intensive to stabilize thermocapillary flow with respect to the adiabatic case [17]. On the other hand, in the range of small Biot number, the critical Marangoni number increases rapidly with decreasing heat-loss, then drops sharply to that of the adiabatic case. This phenomenon is qualitatively consistent with experimental predictions [19] where Wang et al. also found that the critical Marangoni number decreases substantially when the modified average Biot number over the free surface changes from positive to zero.

Noting that the disturbances must vanish at the solid ends, the magnitude of the disturbances near the solid ends should be smaller than in the bulk region. The stability properties of the basic flow are mainly determined by the “effective” temperature difference in the middle part of the liquid bridge [23] where the largest disturbances exist. From this viewpoint, the temperature gradient at the middle part of the free surface was investigated (see Fig. 4). It was discovered that the temperature gradient at the middle part of the free surface increases with increasing Biot number in the range  $Bi \geq 0.4$ . Hence with the same applied temperature difference the effective temperature difference at the middle part of the free surface is larger for the case with larger  $Bi$ , and the corresponding

basic flow tends to be destabilized. On the other hand, according to the boundary condition of the thermal perturbation at the free surface:

$$\vec{n} \nabla T' = -Bi \times T', \tag{10}$$

whenever a positive temperature disturbance arises somewhere on the free surface, it is accompanied by an increase of heat-loss through that part, and vice versa. Therefore, interfacial heat exchange restrains development of the temperature disturbance. To verify these remarks, Fig. 3 also shows the computed results with the  $Bi$  in Eq. (10) (but not in the basic state equations) set to zero. With the same basic flow, the interfacial heat exchange significantly stabilizes thermocapillary flow, and the stabilization effect becomes intensive with increasing Biot number. Practically, the major convex tendency of the  $Ma_c$  profile could be due to competition of the two mechanisms mentioned above. However, the appearance of the local maximum of  $Ma_c$  in the range of small Biot numbers, could not be explained either in experimental studies [15,19] or in the present study. Some interesting phenomena should be noted. One is that the temperature gradient distribution exhibits an undulation at the middle part of the free surface in the range of small Biot number (see Fig. 4). This configuration transition coincidentally corresponds to appearance of the local maximum of the  $Ma_c$  profile. The other phenomenon is a special axisymmetric oscillation mode with azimuthal wave number  $m = 0$  that dominates the peak region of the neutral stability boundary, contrary to the other cases with  $m = 1$ . Fig. 5c shows the corresponding distributions of the velocity and temperature disturbances at the horizontal middle plane  $z = \frac{r}{2}$ . For the  $Bi = 0.3$  case, the axisymmetric nature of the perturbations is obvious. There is no azimuthal velocity disturbance and the other disturbances are equally distributed azimuthally. However, the detailed relationships between the above phenomena and the local maximum of the  $Ma_c$  profile need further investigation.

To better understand energy transfer between the basic thermal field and the temperature disturbance of the thermocapillary flow, the normalized “thermal” energy balance was investigated. In all cases studied, the term  $Q$  which indicates the energy transfer through the free surface is relatively small (in the order of  $10^{-2}$ ). The temperature disturbances on the free surface are strongly restrained. Fig. 5a shows that the radial temperature gradient of the basic thermal field is significant in the center and both the hot and cold corners of the liquid bridge, while the axial temperature

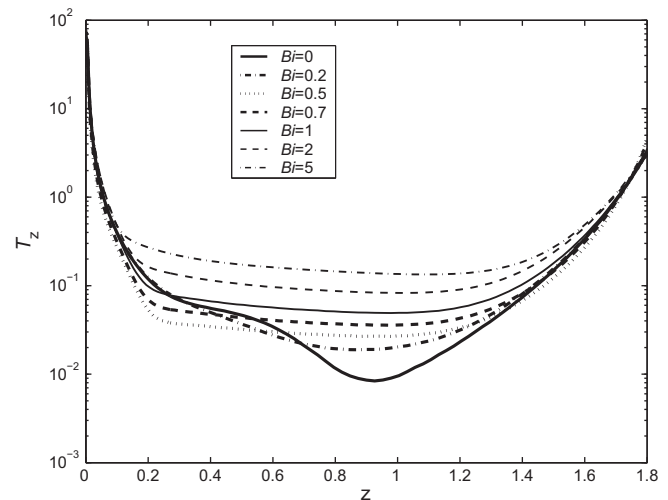
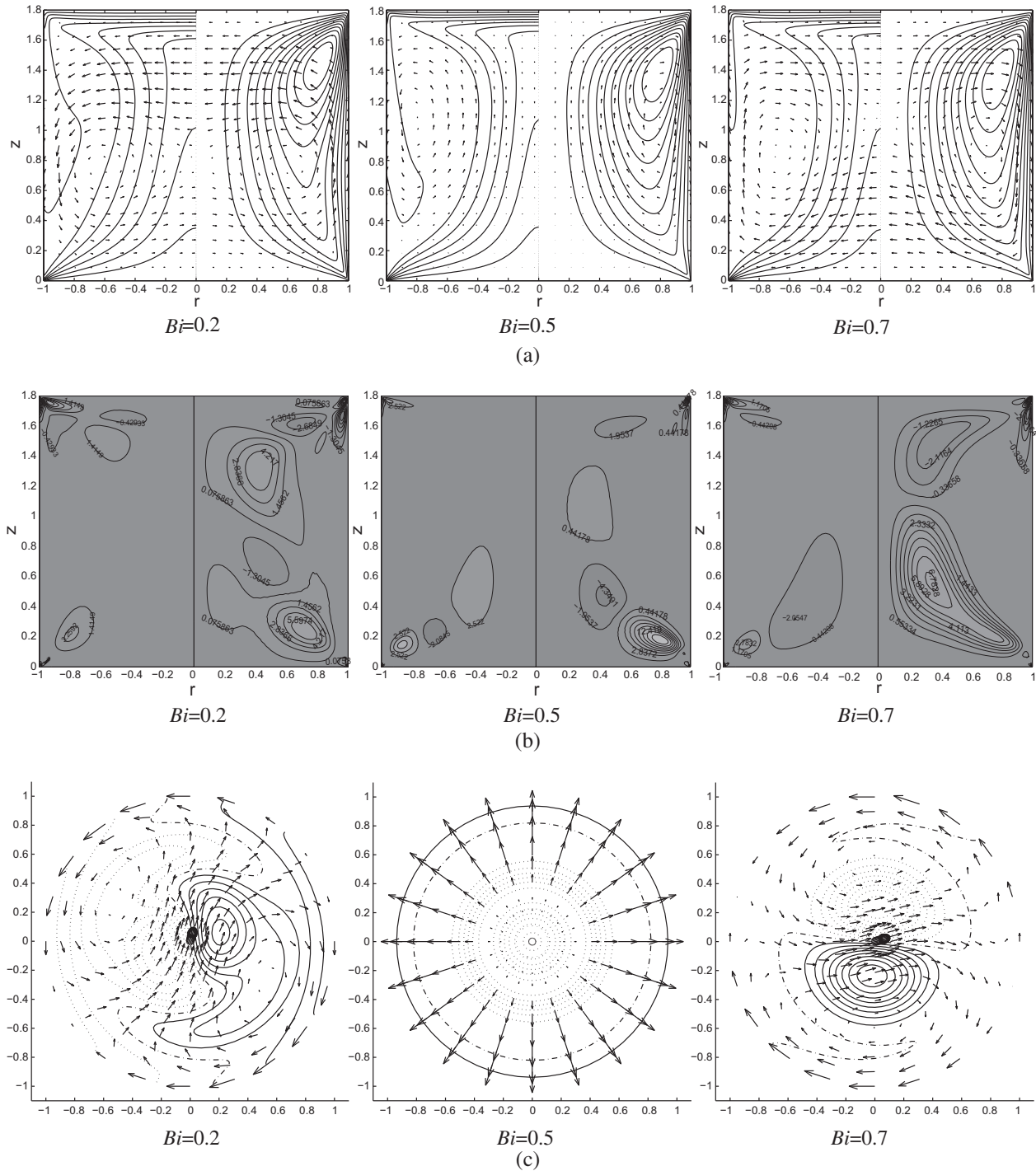


Fig. 6. Biot number dependent temperature gradient distribution at free surface at corresponding  $Ma_c$  for linear  $T_{amb}$ .



**Fig. 7.** (a) Streamlines (solid lines on right) and isothermals (solid lines on left) of the basic steady flow and velocity disturbances (vectors) in  $r$ - $z$  plane; (b) distribution density  $j_1$  (right) and  $j_2$  (left) in  $r$ - $z$  plane; (c) velocity disturbances (vectors) and isolines of temperature disturbances (solid lines: positive temperature disturbance; dotted lines: negative temperature disturbance; dash-dotted line: zero temperature disturbance) at horizontal cut plane  $z = \frac{1}{2}$  at the corresponding critical state at different Biot number for linear  $T_{amb}$ .

gradient is significant in the hot end and cold corner. According to Eq. (9),  $J_1$  is the energy transfer to the temperature disturbance from the radial temperature distribution of the basic thermal field by the radial velocity disturbance, while  $J_2$  is the energy transfer to the temperature disturbance from the axial temperature distribution of the basic thermal field by the axial velocity disturbance. Therefore, for the cases with the oscillatory mode of  $m = 1$  (see Fig. 5b),  $J_1$  has its maximum distribution density in the center of

the liquid bridge, and makes the major contribution to the disturbance energy which always serves as the destabilizing effect.  $J_2$  has its maximum distribution density in the cold corner, and compared to  $J_1$  makes a less important contribution to the disturbance energy. For instance,  $J_1$  is 0.75 and 1.1 for Biot number 0.2 and 0.5 respectively, and correspondingly  $J_2$  is 0.25 and  $-0.1$ , respectively. On the other hand, for the cases with oscillatory mode of  $m = 0$ , in the center of the liquid bridge, the velocity disturbance is nearly

parallel to the basic thermal contours, and both  $J_1$  and  $J_2$  have maximum distribution density in the cold corner. In the case of  $Bi = 0.3$ , for instance,  $J_1$  equals 0.1 and  $J_2$  equals 0.9, so that the major contribution to the disturbance energy is from  $J_2$  instead of  $J_1$ .

Secondly, the case with linearly distributed ambient temperature ( $T_{amb} = z/\Gamma - 0.5$ ) [18] was investigated. In this case, heat-loss to the environment occurs at the lower part of the free surface, while heat-gain occurs from the environment at the upper part. With increasing interfacial heat exchange, the isotherms and streamlines of the two-dimensional axisymmetric convection (not shown) at the corresponding  $Ma_c$  behave quite similarly to the case with the constant ambient temperature ( $T_{amb} = T_{cold}$ ), and likewise for the temperature gradient distributions on the free surface (see Fig. 6). Fig. 3 shows the heat transfer dependent  $Ma_c$ . (Fig. 3 also shows the computed results with  $Bi$  in Eq.(10) set to zero). The  $Ma_c$  profile exhibits a roughly similar tendency to the case with constant ambient temperature, except for the much flattened slope of the profile in the range of large  $Bi$ . Moreover, the special oscillation mode of  $m = 0$  dominates the peak region of the neutral stability boundary, unlike the other cases with  $m = 1$ . Fig. 7 shows the computed results for the disturbances distribution. Similar to the constant ambient temperature case, in the global energy contributions of the terms in Eq. (9), energy transfer through the free surface  $Q$  is relatively small (in the order of  $10^{-2}$ ), while the major contribution to the disturbance energy for the cases of  $m = 1$  is from  $J_1$  which always serves as a destabilizing effect.  $J_2$  also makes a contribution to the disturbance energy, but with less importance compared to  $J_1$ . On the other hand, for the cases of  $m = 0$ , the major contribution to the disturbance energy is from  $J_2$ , and  $J_1$  makes a much smaller contribution to the disturbance energy.

Finally, the effect of the interfacial heat exchange on the thermocapillary flow in liquid bridge of low Prandtl number fluid in microgravity was also studied as a comparison. The details of the physical model and mathematical formulation can be found in [24]. Fig. 8 shows the computed results for a liquid bridge ( $\Gamma = 2.0$ ) of molten tin ( $Pr = 0.009$ ). The melting point of tin is 750 K. The ambient temperature is assumed to be 300 K, hence thermal radiation ( $\varepsilon$  is assumed to be 0.1) plays the major role in interfacial heat exchange in this case. With the adiabatic melt free surface, the critical Reynolds number is determined as  $Re_c = 2819$  with critical oscillation frequency  $f_c = 0.468$  Hz. When interfacial radiation is taken into account the critical Reynolds number is determined as  $Re_c = 2828$  with  $f_c = 0.474$  Hz. The deviation between the critical Reynolds numbers is less than 1%. Consequently, unlike the case of the liquid bridge of high Prandtl number fluids, the effect of interfacial heat exchange on the onset of oscillatory thermocapillary flow in a liquid bridge of low Prandtl number fluids in microgravity is insignificant.

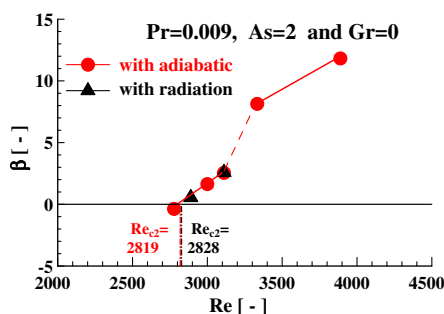


Fig. 8. Critical Reynolds number for liquid bridge of  $Pr = 0.009$  with adiabatic and radiative free surface.

## 4. Conclusions

The effect of interfacial heat exchange on the onset of oscillatory thermocapillary flow in a cylindrical liquid bridge formed by 1 cst silicone oil ( $Pr = 16.0$ ) with aspect ratio 1.8 in microgravity was investigated in an extended range of Biot number. With both constant and linearly distributed ambient temperatures, the computed results predict that interfacial heat exchange plays an important role in oscillatory thermocapillary flow in liquid bridges of high Prandtl number fluids. The corresponding marginal stability boundary exhibits a roughly convex trend with increasing Biot number. However, a sharp local maximum exists in the range of small Biot number where a special oscillation mode of  $m = 0$  dominates, contrary to the other cases with  $m = 1$ . For the case of  $m = 1$ , the major destabilizing contribution to the disturbance energy is from the energy transfer from the radial temperature distribution of the basic thermal field in the center of the liquid bridge by the radial velocity disturbance. For the case  $m = 0$  the major destabilizing contribution is from the energy transfer from the axial distribution of the basic thermal field in the cold corner of the liquid bridge by the axial velocity disturbance. Moreover, the effect of interfacial heat exchange on thermocapillary flow in a liquid bridge of low Prandtl number fluid in microgravity was also investigated as a comparison, and predicted to be insignificant.

## Acknowledgments

This research is supported by the National Natural Science Foundation of China (Grant Nos. 11032011, 10872202) and the Knowledge Innovation Project of the Chinese Academy of Sciences (Grant No. KJCX2-YW-L08).

## References

- [1] W.R. Hu, Z.M. Tang, K. Li, Thermocapillary flow in floating zones, *Appl. Mech. Rev.* 61 (2008) 010803-15.
- [2] Ch.H. Chun, W. Wuest, A micro-gravity simulation of the Marangoni convection, *Acta Astronaut.* 5 (1978) 681–686.
- [3] Ch.H. Chun, W. Wuest, Experiments on the transition from the steady to the oscillatory Marangoni-convection of a floating zone under reduced gravity effect, *Acta Astronaut.* 6 (1979) 1073–1082.
- [4] D. Schwabe, A. Scharmann, F. Preisser, R. Oeder, Experiments on surface tension driven flow in floating zone melting, *J. Cryst. Growth* 43 (1978) 305–312.
- [5] D. Schwabe, A. Scharmann, Some evidence for the existence and magnitude of a critical Marangoni number for the onset of oscillatory flow in crystal growth melts, *J. Cryst. Growth* 46 (1979) 125–131.
- [6] M.K. Smith, S.H. Davis, Instability of dynamic thermocapillary liquid layer Part I: Convective instability, *J. Fluid Mech.* 132 (1983) 119–144.
- [7] G.P. Neitzel, K.T. Chang, D.F. Jankowski, H.D. Mittelmann, Linear stability of thermocapillary convection in a model of the floating zone crystal growth process, *AIAA* 92 (1992) 0604.
- [8] M. Wanschura, V.M. Shevtsova, H.C. Kuhlmann, H.J. Rath, Convective instability mechanisms in thermocapillary liquid bridge, *Phys. Fluids* 7 (1995) 912–925.
- [9] G. Chen, A. Lizee, B.J. Roux, Bifurcation analysis of the thermocapillary convection in cylindrical liquid bridge, *J. Cryst. Growth* 180 (1997) 638–647.
- [10] C.H. Nienhüser, H.C. Kuhlmann, Stability of thermocapillary flows in non-cylindrical liquid bridges, *J. Fluid Mech.* 458 (2002) 35–73.
- [11] G.P. Neitzel, C.C. Law, D.F. Jankowski, H.D. Mittelmann, Energy stability of thermocapillary convection in a model of the floating zone crystal growth process, *Phys. Fluids A* 3 (1991) 2841–2846.
- [12] R. Savino, R. Monti, Oscillatory Marangoni convection in cylindrical liquid bridge, *Phys. Fluids* 8 (1996) 2906–2922.
- [13] V.M. Shevtsova, J.C. Legros, Oscillatory convection motion in deformed liquid bridges, *Phys. Fluids* 10 (1998) 1621–1634.
- [14] M. Levenstam, G. Amberg, C. Winkler, Instability of thermocapillary convection in a half-zone at intermediate Prandtl numbers, *Phys. Fluids* 13 (2001) 807–816.
- [15] Y. Kamotani, L. Wang, S. Hatta, A. Wang, S. Yoda, Free surface heat loss effect on oscillatory thermocapillary flow in liquid bridges of high Prandtl number fluids, *Int. J. Heat Mass Transfer* 46 (2003) 3211–3220.
- [16] M. Irikura, Y. Arakawa, I. Ueno, H. Kawamura, Effect of ambient fluid flow upon onset of oscillatory thermocapillary convection in half-zone liquid bridge, *Microgravity Sci. Technol.* 16 (2005) 176–180.

- [17] D.E. Melnikov, V.M. Shevtsova, Thermocapillary convection in a liquid bridge subjected to interfacial cooling, *Microgravity Sci. Technol.* 18 (2006) 128–131.
- [18] Y. Kousaka, H. Kawamura, Numerical study on the effect of heat loss upon the critical Marangoni number in a half-zone liquid bridge, *Microgravity Sci. Technol.* 18 (2006) 141–145.
- [19] A. Wang, Y. Kamotani, S. Yoda, Oscillatory thermocapillary flow in liquid bridges of high Prandtl number fluid with free surface heat gain, *Int. J. Heat Mass Transfer* 50 (2007) 4195–4205.
- [20] B. Xun, K. Li, P.G. Chen, W.R. Hu, Effect of interfacial heat transfer on the onset of oscillatory convection in liquid bridge, *Int. J. Heat Mass Transfer* 52 (2009) 4211–4220.
- [21] G.H. Golub, C.F. VanLoan, *Matrix Computations*, Johns Hopkins University Press, Baltimore, 1996.
- [22] B. Xun, P.G. Chen, K. Li, Z. Yin, W.R. Hu, A linear stability analysis of large-Prandtl-number thermocapillary liquid bridges, *Adv. Space Res.* 41 (2008) 2094–2100.
- [23] D. Schwabe, Hydrothermal waves in a liquid bridge with aspect ratio near the Rayleigh limit under microgravity, *Phys. Fluids* 17 (2005) 112104.
- [24] N. Imaishi, S. Yasuhiro, Y. Akiyama, S. Yoda, Numerical simulation of oscillatory Marangoni flow in half-zone liquid bridge of low Prandtl number fluid, *J. Cryst. Growth* 230 (2001) 164–171.